Review Article

Circularly Polarized Luminescence: A Review of Experimental and Theoretical Aspects

GIOVANNA LONGHI,[1] ETTORE CASTIGLIONI,[1,2] JUN KOSHOUBU,[3] GIUSEPPE MAZZEO,[1] AND SERGIO ABBATE[1]*

[1]*Department of Molecular and Translational Medicine, Università di Brescia, Brescia, Italy*
[2]*JASCO Europe, Cremella (LC), Italy*
[3]*JASCO Corporation, Ishikawa-machi, Hachioji, Tokyo, Japan*

ABSTRACT We review the present status of experiments and calculations for circularly polarized luminescence (CPL) of simple organic molecules and of stimuli-responsive organic molecules. Together with the historical report of the main instrumental approaches, a few crucial points about experiments are tackled, with the aim of defining measurement protocols, in view of the wide availability of commercial apparatuses in the near future. The calculations aimed at interpreting the CPL spectra, mostly based on time-dependent Density Functional Theory (TD-DFT) calculations, which started around 2010, are reviewed, limiting the discussion to small to mid-sized molecules. Some applications of CPL spectra of organic molecules-based systems are presented, with a focus especially on two fields: material science and biology. *Chirality 28:696–707, 2016.*

KEY WORDS: circularly polarized luminescence (CPL); material science; applications in biochemistry; TD-DFT calculations; vibronic effects; fluorescence and phosphorescence

To the best of our knowledge, circularly polarized luminescence (CPL) was first measured in 1948 by Samoilov[1] on a chiral crystal of sodium uranyl acetate and was more actively pursued in 1960 by Oosterhoff and the Dutch school;[2] from then on, a number of articles appeared with a constant production of about 10 articles per year until 2010. Afterwards, a constant increase of articles is recorded, with the number of articles per year being close to 100 and increasing (see Appendix). Coming to a brief history of the matter introduced above, the basis of the CPL technique was established by Emeis and Oosterhoff.[2,3] Measurements were carried out by rotating manually a quarter wave-plate and later on by rotating it continuously with phase-sensitive detection; the Dutch school, especially Meskers and Dekkers, kept improving the technique.[3] A comprehensive review can be found in Ref. 4. Just a few years later, at the Weizmann Institute, Steinberg and Gafni[5] developed their own instrumentation and studied in particular molecules of biological interest. In the USA Richardson was the first, to our knowledge, to develop the technique.[6] In that school Jim Riehl, Harry Brittain, and Gilles Muller are worth mentioning, having written a number of important articles and several reviews, among which we mention Refs. 7–10. Last but not least, in this historical reconstruction one cannot forget that numerous important CPL works appeared in Japan, as will become clear below, the first one to our knowledge is reported in Ref. 11.

With respect to the two recent reviews, by Zinna and Di Bari[12] and by de la Moya et al.,[13] the first one dealing with the CPL of lanthanide complexes and the second one dealing with comparison of CPL of various organic molecules, the aim of this work is to focus on the following three aspects. 1) experimental aspects (instrument design and measurement protocols) already stressed to some extent in a previous article;[14] 2) presentation of applicative potentialities of CPL to particular organic systems, used in material science and biology; and 3) the most recent theoretical/computational approaches to the interpretation of CPL spectra, based on time-dependent Density Functional Theory (TD-DFT), a method employed since 2010. Illustrative examples are provided regarding the three aspects.

We finish these introductory notes by presenting a few examples of why CPL is so fascinating: in 1980 Wynberg et al.[15] reported the intriguing bio-chemiluminescence phenomenon that the left and right lanterns of two firefly species (Photuris lucicrescens and Photuris versicolor) emit circularly polarized light of opposite sense (see Fig. 1a); a proposed interpretation of the phenomenon is birefringence: even though their constituent molecules are of the same chirality, they may be viewed as mirror image macroscopic meso-structures.[15] Additional phenomena, where CPL manifests and is potentially useful, are presented in Figure 1b, where CPL is observed in Quantum Dots[16,17] with Laser etching response, and in Figure 1c,[18] where CPL was found in standard PMMA-based polymeric material, treated in such a way as to host chiral guest molecules. Other interesting examples for possible analytical applications of CPL are presented in Figure 2 and demonstrate CPL's extreme sensitivity to either anions[19,20] or cations[21] (evidence for the latter is presented in the supplementary material of Ref. 21) and also to pH[22] (sensitivity to cations is reported also in Ref. 23).

*Correspondence to: S. Abbate, Department of Molecular and Translational Medicine, Università di Brescia, Viale Europa 11, 25123 Brescia, Italy. E-mail: sergio.abbate@unibs.it
Received for publication 25 June 2016; Accepted 26 August 2016
DOI: 10.1002/chir.22647
Published online in Wiley Online Library (wileyonlinelibrary.com).

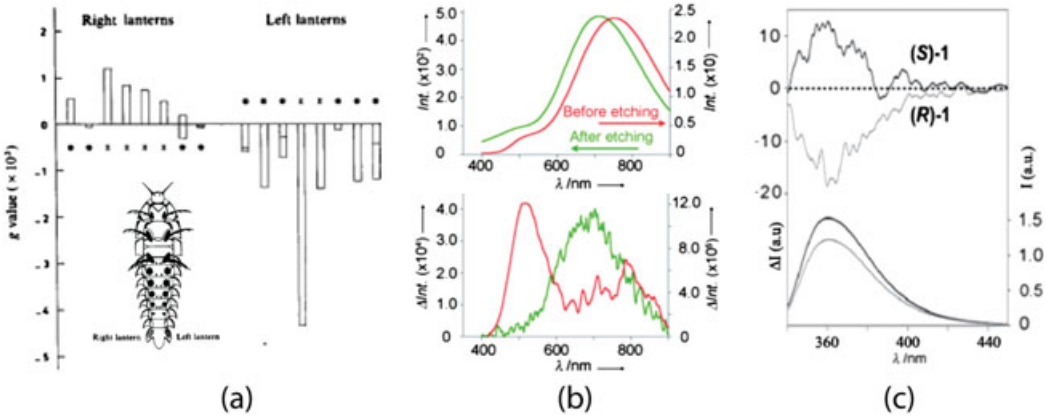

Fig. 1. Applications of CPL. (**a**) bio-chemoluminescence dissymmetry factor of right and left lanterns of a common firefly (adapted from Wynberg et al.[15]). (**b**) Fluorescence (top) and CPL spectra of CdS@Ferritin Quantum dots before and after Laser etching (adapted from Naito et al.[16]). (**c**) CPL (top) and PL (lower) spectra of (*S*)- and (*R*)-Binaphtols as dopants of PMMA (adapted from Kimoto et al.[18]).

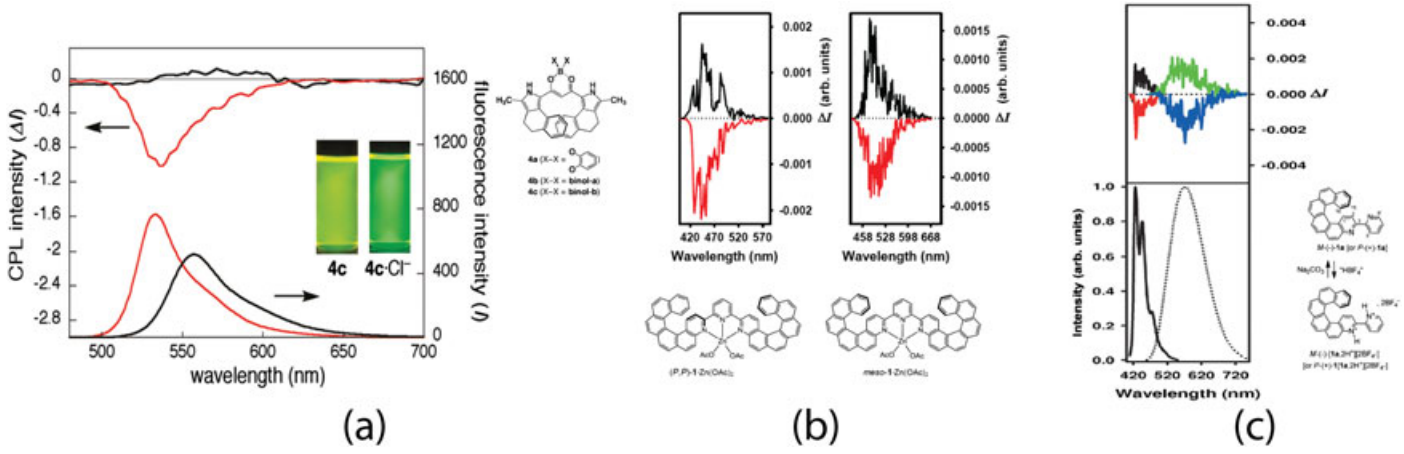

Fig. 2. CPL of ion- and pH-sensitive active systems: anion-responsive (**a**), cation-responsive (**b**), and pH-sensitive (**c**). Data taken from Refs. 19,21,22, respectively.

Many more interesting applications of CPL than presented above have been reported in the literature, and a small sample of quite recent contributions, mainly from several laboratories in Japan, may be found in Refs. 24–31.

EXPERIMENTAL ASPECTS

CPL is defined and is often measured as $(I_L\text{-}I_R)$, i.e., the intensity difference of left and right circularly polarized radiation emitted by the sample, the average emitted intensity being $(1/2)(I_L + I_R)$; sometimes it is measured in terms of the dissymmetry factor: $g_{lum} = (I_L - I_R)/[(1/2)(I_L + I_R)] = \Delta I/I$. This can be achieved in different ways; in case of strong signals ($g_{lum} \sim 1$) simple achromatic quarter wave plates are enough, in strong analogy of what was done in the early days of CPL.[1,2] However, most chiral samples, like organic molecules, polymers, or biochemical systems, exhibit low values for g_{lum}, on the order of 10^{-2} to 10^{-3}. For such samples sensitivity is poor and one must resort to the use of an electro-optic or photoelastic light modulator (PEM).[5] The latter scheme is the one that was implemented in our apparatus.[32] Before coming to the presentation of some selected features of our instrument, let us observe that recent trends in the evaluation of new materials focus on maximizing g_{lum}, and in this case units based on PEM modulation may offer limited range.[33] In addition, soon it was also discovered that linearly polarized components due to photoselection may leak into the CPL signal, distorting the data.[34] These effects may be minimized by exciting the sample with fully unpolarized radiation, when using forward or backscattering geometries, or by inserting a linear polarizer in the excitation path, parallel to the direction of the collected beam, with the more conventional 90° approach. Concerning the use of photoelastic modulators, several approaches are possible: lock-in amplifiers, as in the case of circular dichroism CD, photon counting intensity measurements, or more simply direct intensity evaluation of the demodulated signals; however, there is not a clear indication of the relative advantages of the different approaches. In our home-built apparatus, for which we report a scheme and a picture in Figure 3, we employ a lock-in amplifier to demodulate the signal, and this, among other advantages, tied to the design of the instrument, gives an advantage related to intensity scale calibration. For this matter, while there is a general consensus toward employing Eu(facam),[14] even the absolute values reported in the literature do not agree precisely;[4] thus, our approach allows calibrating the scale with a known CD standard irradiated in forward mode by a "white" LED and this method turns out to be simple and effective. The LED is placed at 180° and the system is operated in automatic dynode feedback mode, which keeps the DC signal at a constant value (1 volt in our case), allowing us to obtain regular CD spectra. CD is measured as $(A_L\text{-}A_R)/[(1/2)(A_L + A_R)] = AC/DC$, as ellipticity θ(mdeg) for the unitary DC value. With due cautions described in Ref. 32, we recorded the visible CD spectrum of Δ-(−)-$Co(en)_3I_3H_2O$ in water, measuring the intensity of the 490nm band. The same calibration procedure is then used directly for the CPL measurements, where our instrument allows one to measure ΔI as ellipticity (θ) in mdeg and I in volts.

Let us point out a few features of Figure 3, which are instrumental to the discussion of this review. The "reverse" CD design, the usefulness of which has just been pointed out; the possibility of employing several sources, providing thus several geometries for irradiation as well as for

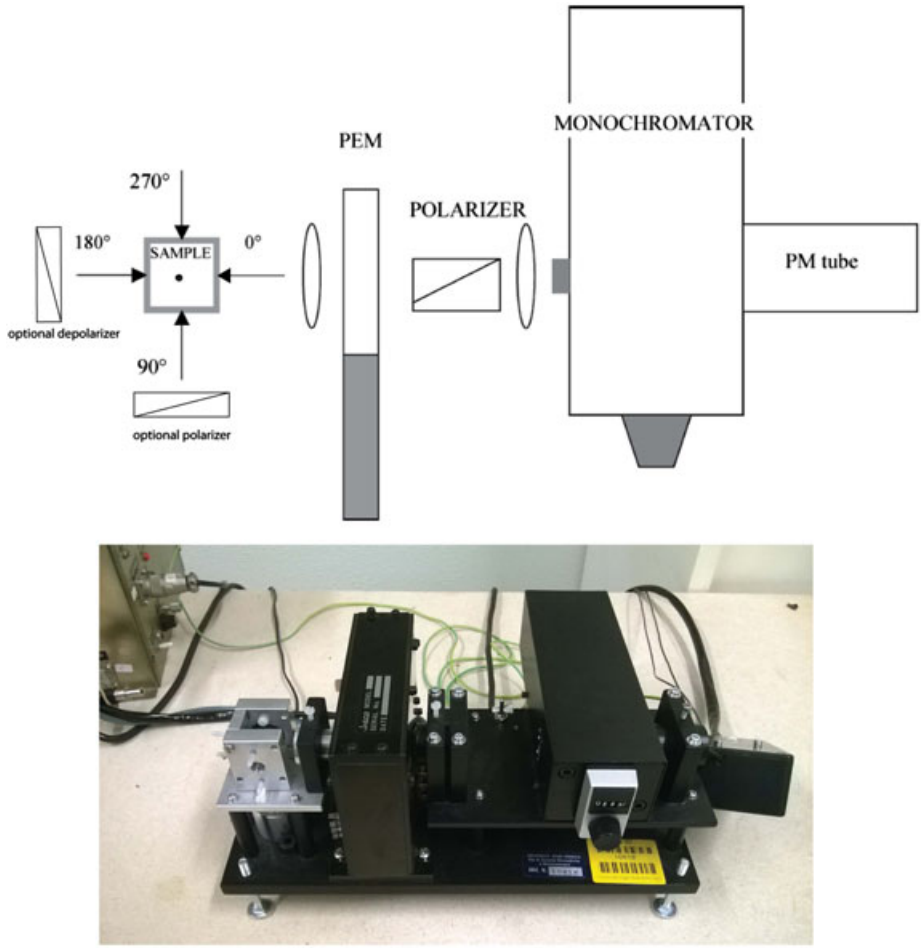

Fig. 3. Top: layout of the home-built CPL apparatus at the University of Brescia. Lower: a picture thereof (Ref. 32).

collection; the possibility of inserting either polarizers or depolarizers, for the reasons expounded above; or for possible additional difficulties posed by samples (mainly in the solid state). In most experiments we employ radiation from a fluorimeter located nearby, brought to the sample with a water-filled waveguide. One last and simple, but in any case quite useful feature of our apparatus, is the possibility to simultaneously record the fluorescence (as DC signal) and the CPL spectra (as demodulated AC signal). This feature is essential to provide a reliable g_{lum} factor at variable wavelength.

Another CPL apparatus recently used, produced by JASCO (Tokyo, Japan) as CPL-300, employs prisms. The optical configuration is the same as that of our home-built one except for the fluorescence monochromator being set parallel to the excitation light azimuth (180° geometry). The prism system has the following two important abilities. One is the high CPL detection ability, especially for the visible and the ultraviolet region.[35] The other is that the CPL spectrum is stray light-free, high-order light-free, and grating anomaly-free. On the other hand, 180° geometry makes it easy to adjust the CPL scale using a CD standard sample. This is achieved by setting the wavelengths on the emission side and the excitation side at the same value. In this review article, we focus on the experimental applications obtained by using the home-built CPL apparatus.

Let us now describe the protocol for taking CPL spectra, which we strongly advise. 1) First, collect the CD and absorbance spectra in the same cell to be used in the CPL experiment, in order to decide the proper sample concentration. 2) Run a quick fluorescence spectrum on a fluorimeter, to confirm emission wavelength and intensity and/or run excitation spectrum to improve wavelength excitation. 3) Run CPL spectra with a single or multiple scans. 4) At the end of the procedure, rerun a CD spectrum, in order to verify whether degradation of the sample has occurred (this is quite common).

Careful attention should be paid to possible contributions altering the pure CPL phenomenon. Irradiation of sample with linearly polarized light gives origin to photoselection, since absorption probability is higher for molecules with an electric dipole transition moment parallel to the polarization direction. Since linearly polarized components in a birefringent medium generate elliptical polarization, one then obtains CPL artifacts. All this suggests, when adopting the forward geometry, the use of depolarized excitation light, and, when adopting instead a 90° geometry, the use of linearly polarized excitation parallel to the direction of the collected emitted beam. In this case g_{lum} is simply a function of the isotropic rotational and dipole strengths. For solid samples and for viscous media, measuring linearly polarized luminescence is essential.

When scattering phenomena are important, chiral scattering may manifest itself as apparent CPL: an example regarding chiral fibrils will be discussed below.

Finally, we wish to warn CPL utilizers that one may incur some problems if fluorescence (and CPL) is too close in wavelength to absorption (and CD). In that case the observed CPL needs be corrected, since part of the emitted radiation may be reabsorbed and the reabsorption is different for right circularly polarized and left circularly polarized light. In Ref. 36 we derived a couple of correction equations for fluorescence and for CPL, which we repeat here:

$$Fluo_{corr} = \frac{Fluo_{obs}}{T}$$

$$CPL_{corr} = \frac{1}{T} Fluo_{obs} \left(\alpha^* \ln(10) * \ \Delta A \right) + \frac{1}{T} (CPL_{obs}) =$$

$$CD_{term} + CPL_{term}$$

In the above equations $Fluo_{obs}$ and CPL_{obs} are the actually observed fluorescence and CPL signals, respectively, the first one being contaminated by absorbance (A) or, equivalently, by transmittance (T), the second one being affected by T and circular dichroism (ΔA). The above formulae permit one to arrive at the genuine molecular phenomena of fluorescence ($Fluo_{corr}$) and of CPL (CPL_{corr}). Finally, for ease of presentation of the results in Figure 4, we named the two terms of the second equation as CD_{term} and CPL_{term}. One needs additionally to know the geometrical factor α, which is related to the experimental geometry and to the employed cuvette (in the case we proposed in Ref. 36, α = 2.5, since the cuvette was 2 x 10 mm and we assumed the phenomenon to take place mainly (or on average) at the center of the cuvette). Please notice that all data reported in this review article were obtained with the apparatus presented in Figure 3, with few exceptions recalled in the figure captions.

We report in Figure 4 measurements conducted on poly-[3-((*S*)-2-methylbutyl)-thiophene] in mixed solvent solutions. In this case the autoabsorption effect is particularly dramatic and the correction appears to be quite necessary; we were also driven to introduce such correction by observing that the sign of the observed CPL signal was opposite to the sign of the longest wavelength CD band, a quite uncommon event (vide infra).

EXAMPLES OF THE USE OF CPL SPECTRA FOR ORGANIC-BASED SYSTEMS

In this section we present a few examples that evidence the importance of CPL data in investigating either fine details of the nature of the first excited state of organic molecules or of aggregation phenomena or of supramolecular phenomena, which CPL brings to light. We start out in Figure 5 with examples of (*R*) and (*S*)-camphor, of (*R*) and (*S*)-camphorquinone, and of (1*S*)-5-oxocamphor.[37] We chose these examples because camphor appears rather as a counterexample to the general rule, according to which one should expect (and in most cases one observes) just one CPL band and this band

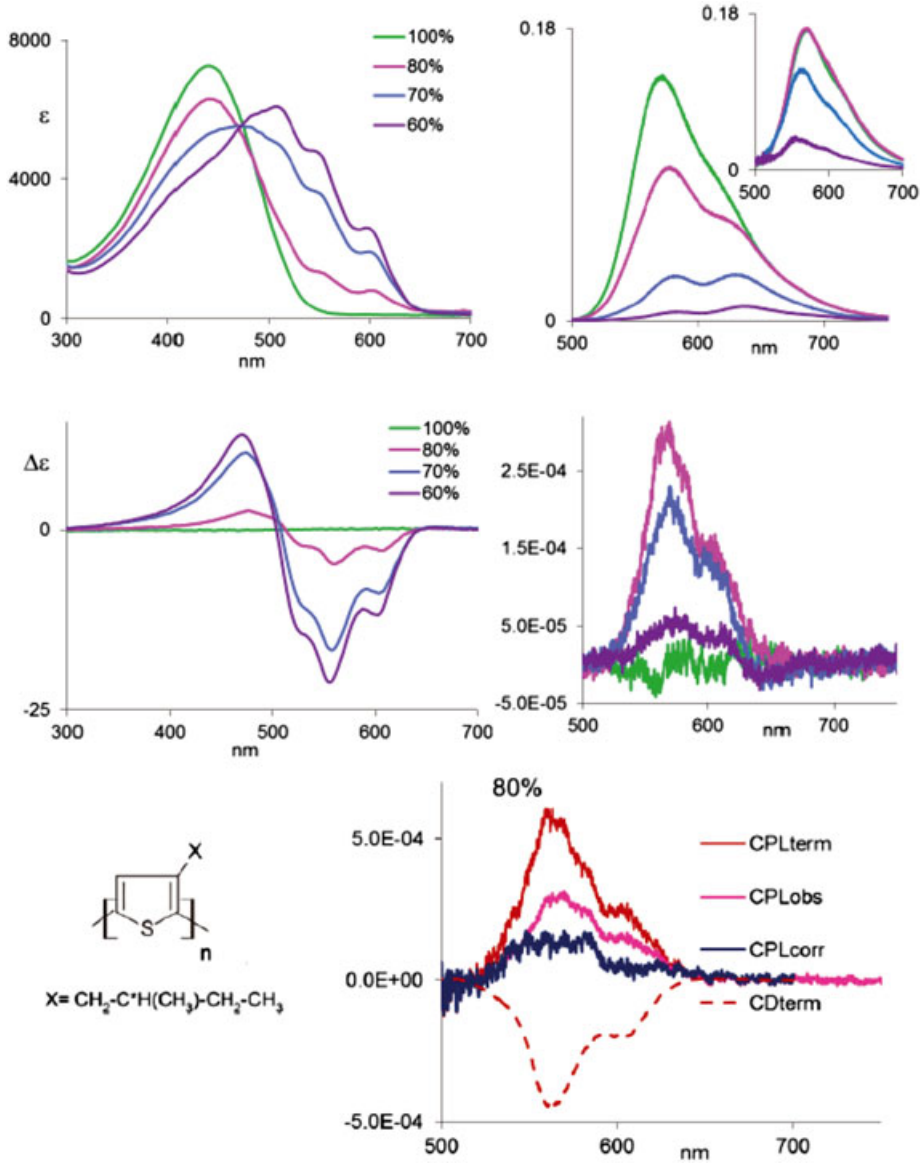

Fig. 4. Absorption (top left), ECD (middle left), fluorescence (top right), and CPL (middle right) recorded spectra of Poly-[3-((*S*)-2-Methylbutyl)-Thiophene] at various $CHCl_3$/butanol mixtures (v/v). The inset in the top right panel shows the corrected fluorescence (see text). Lower panel: For the case of $CHCl_3$/butanol 80% (v/v) the corrected pure CPL contribution (CPL_{corr}) is reported, together with the recorded CPL spectra (CPL_{obs}): the correction is obtained taking into account absorption, fluorescence, and ECD data (also the two terms reported in the text are plotted). (see text and Ref. 36).

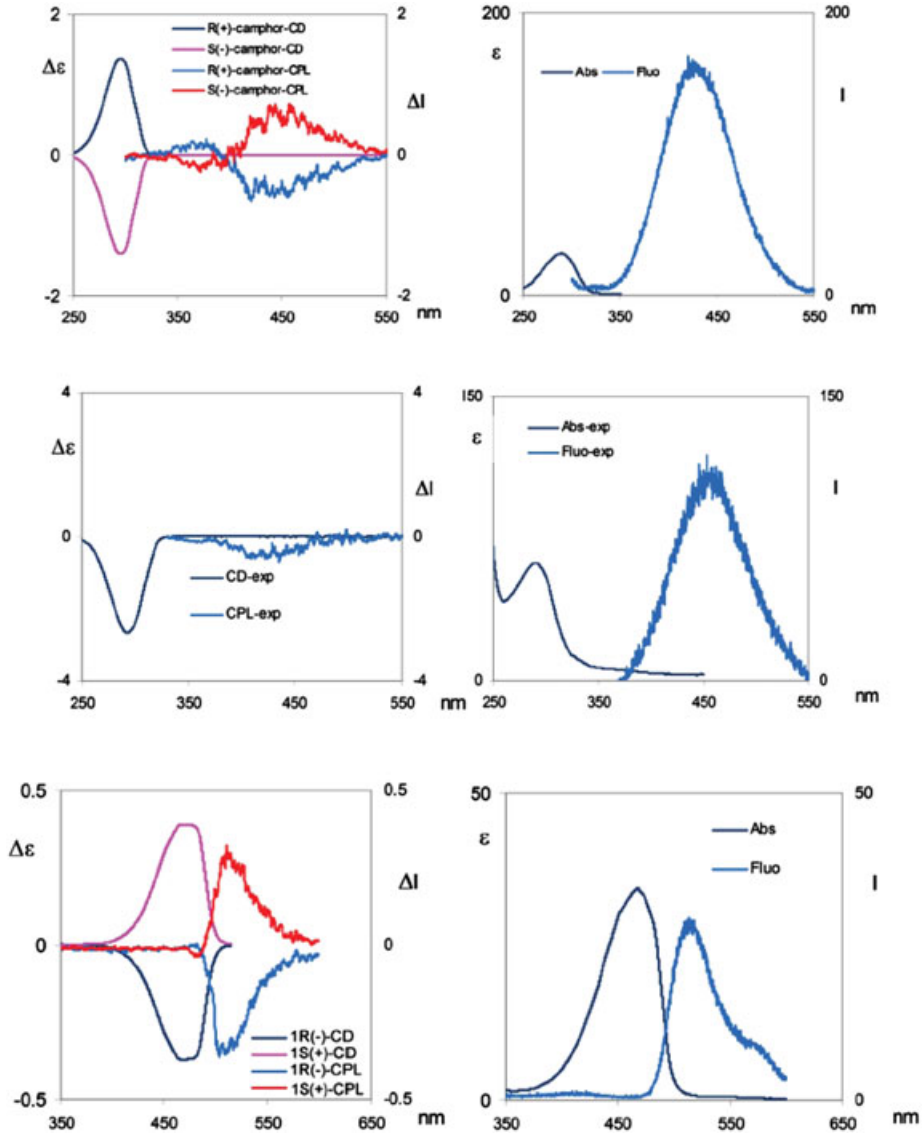

Fig. 5. ECD and CPL (left) and absorption and fluorescence spectra of (*R*)- and (*S*)-1-camphor (top), (1*S*)-5-oxocampor (middle), and (*R*)- and (*S*)-camphorquinone (bottom) (Ref. 37).

has the same sign as the lowest energy CD band. Indeed, according to Kasha's rule,[38] luminescence proceeds from the lowest energy excited electronic state: if this is a singlet S_1 state, the same dipole transition moments (either electric or magnetic) are expected to govern the phenomena of both CD and CPL.[39–42] This is indeed observed in (*R*) and (*S*)-camphorquinone and in (1*S*)-5-oxocamphor. In camphor, instead, two CPL bands of opposite sign are observed and the DFT calculations presented in Ref. 37 allow gaining insight into the excited state to an unexpected degree of finesse, as will be expounded in the next section.

Looking at Figure 6 we may discuss the next example: therein one may appreciate the dependence of CPL on the molecule being either a monomer or a dimer, and in the latter case either an "open" dimer or a dimer forming a ring. We present the case of (*R*) and (*S*)-2,2′-bis(2,2′-bithiophene-5-yl)-3,3′-bithianaphthene (which we abbreviate as (*R*) and (*S*)-T4-BT2). Optical characterization of this compound[43] is of interest for material science, since after electrochemical polymerization on an electrode it shows very good chiral recognition properties under voltammetric cycles.[44,45] On the left we report the CD and CPL spectra for (*S*)-T4-BT2 in monomeric form. In the central part of the figure one has the corresponding CD and CPL spectra for the chemically synthesized "open" dimer of both (*R*) and (*S*)-T4-BT2 (in a previous work,[44] where electrochemical polymerization was carried out, no control of the multiplicity or shape of the polymers was possible). In the right part one has the CD and CPL spectra of the "closed" (*R*) and (*S*)-T4-BT2 dimer, where the authors[45] had made sure that one had a ring-type closed molecule. We may observe that similar sensitivity to the molecule being in the monomeric or dimeric state is exhibited both by CD and CPL; besides, the single CPL band has the same sign as the lowest-energy CD band, in accordance with the most common occurrences. The ratio $|g_{lum}|$ of the T4-BT2 monomer is ca. 10^{-2}, a pretty big value for organic molecules.[13,43] The open dimer of T4-BT2 has $|g_{lum}| \leq 10^{-3}$; the closed dimer has a larger $|g_{lum}| \sim 2\times10^{-3}$.

Another example of the application of CPL spectroscopy is the study of cage-type molecules in organic solvents.[46,47] In Figure 7 one may observe both the CD and the CPL spectra of a cryptophane molecule in CH_3CN. From CPL and

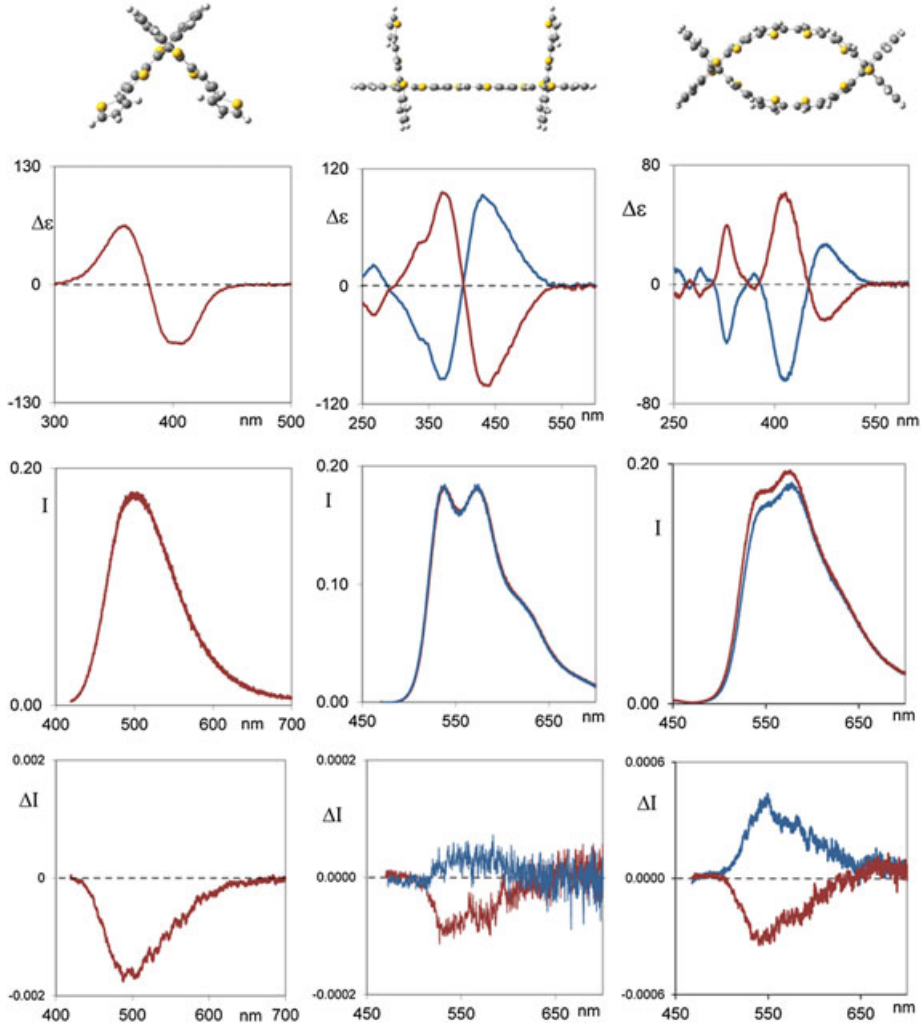

Fig. 6. Left column: CD (top) fluorescence (middle), and CPL spectra of (*R*) -2,2′-bis(2,2′-bithiophene-5-yl)-3,3′-bithianaphthene [(*R*)-(−)-T4-BT2]. Middle column: CD, fluorescence, and CPL spectra of the "open" dimers of (*R*)-(−)-T4-BT2 (red trace) and (*S*)-(+)-T4-BT2 (blue trace). Right column: CD, fluorescence, and CPL spectra of the "closed" dimers of (*R*)-(−)-T4-BT2 (red trace) and (*S*)-(+)-T4-BT2 (blue trace). (Data on left column: from Ref. 43. Data on center column: original new data. Data on right column: from Ref. 45.)

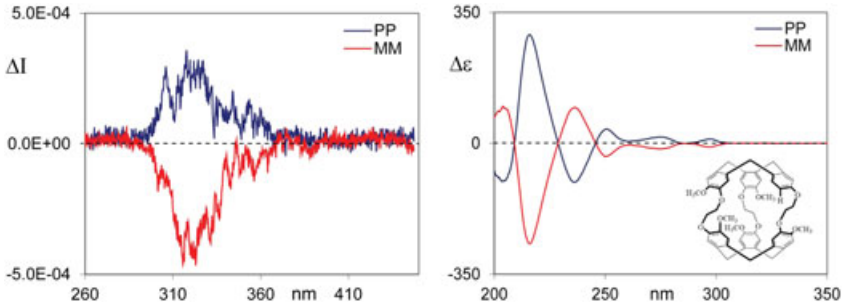

Fig. 7. CPL (left) and ECD spectrum (right) of cryptophanes *MM* and *PP* in 1.5 x 10^{-4} M CH_3CN solution, excitation wavelength 275 nm, CPL is referred to a normalized fluorescence spectrum (original spectra).

fluorescence data we see that $|g_{lum}|$ is of the order of 10^{-4}, among the lowest values that we have been able to record.

So far we have presented examples which are interesting for the field of material science. CPL properties can be studied also for organic systems useful for "soft" material science, and then we slowly move into the field of biology. In Figure 8 let us consider the case of tricarboxamide molecules,[48] a Y-shaped molecule with three long arms and endowed with C_3-symmetry, carrying chiral substituents at the terminal of each arm. Symmetry is not modified by this substitution; in some solvents (methylcyclohexane [MCH in the figure]) they form organogels, in others (chloroform) they do not. Correspondingly, one notices increased CD spectra, a bathochromic shift of the fluorescence band, which also changes shape, but, most notably, the appearance of CPL, which was not observed in chloroform solution. CPL activity

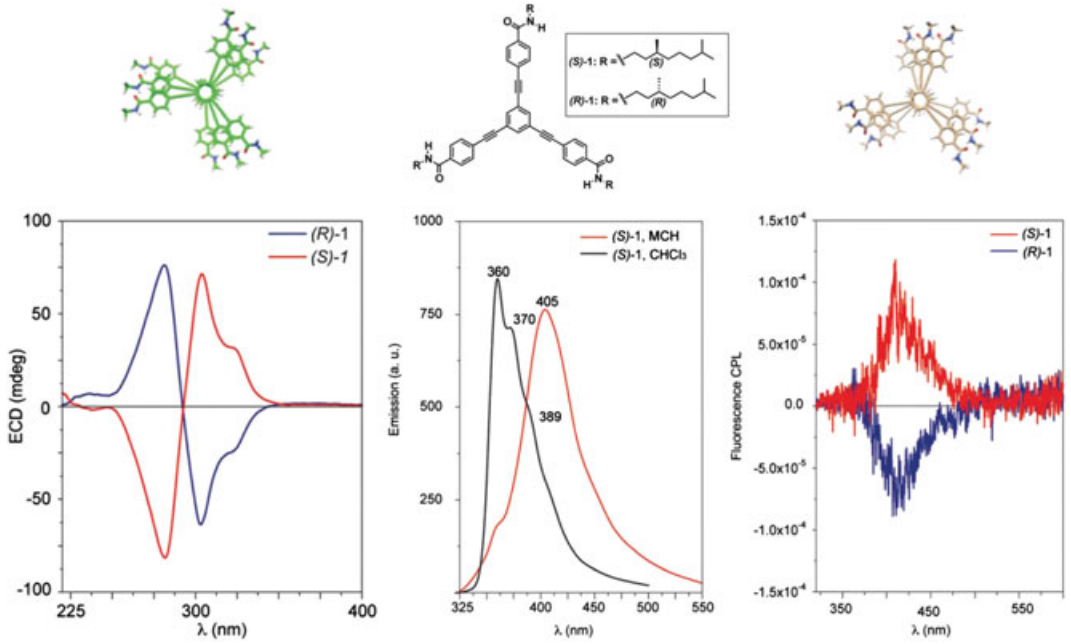

Fig. 8. CD (left), emission (center), and CPL spectra of (*S*)- and (*R*)-tricarboxamides, whose chemical structure is reported in the center top part of the figure. In chloroform they aggregate to provide *P* supramolecular structures (green top) and *M* supramolecular structure (yellow, top) (data taken from Ref. 48).

is ascribed to the formation of columnar tricarboxamide aggregates, which in the end confers to the macroscopic system the aspect of a gel. The gel phase (obviously in water and not organic solvent) is the standard state of the inside of a cell.[49]

In the next example we deal with an achiral molecule thioflavin-T, which was demonstrated to exhibit induced CD in presence of specially prepared insulin fibrils, forming bundles with a left-handed (*M*) or right-handed (*P*) supramolecular assembly.[50] The effect of induced CPL is much more evident,[51] with $|g_{lum}|$ ratios up to 10^{-2}, while $|g_{abs}|$ is between 10^{-3} and 10^{-2} (Fig. 9). It is also notable that the CPL data were obtained in different conditions with forward scattering geometry or at 90° and within a medium with refractive index matching, namely, in methyl salicylate, a liquid with a refractive index comparable to the one of insulin fibrils. Quite similar results were obtained in all conditions. The molecular mechanism whereby thioflavin-T acquires chirality (and also fluorescence activity, since fluorescence is very low in water) is not fully clear, whether it is due to a distortion around the bond connecting the phenyl to the benzo-imidazole moiety or to the interaction with aromatic amino acid units in the protein: DFT calculations admit both possibilities.[51,52]

Finally, we report CPL from a very popular protein used in imaging techniques: green fluorescent protein (GFP),[53,54] for which CD was reported some time ago.[55] In Figure 10 we provide the CD and CPL spectra of GFP in water.[35] We expect that important applications may be generated from this preliminary observation.

CALCULATION OF CPL SPECTRA

Prior to the advent of TD-DFT, the calculation of CPL spectra was not quantitative and dealt with understanding qualitative, yet of fundamental importance, features tied with sign,

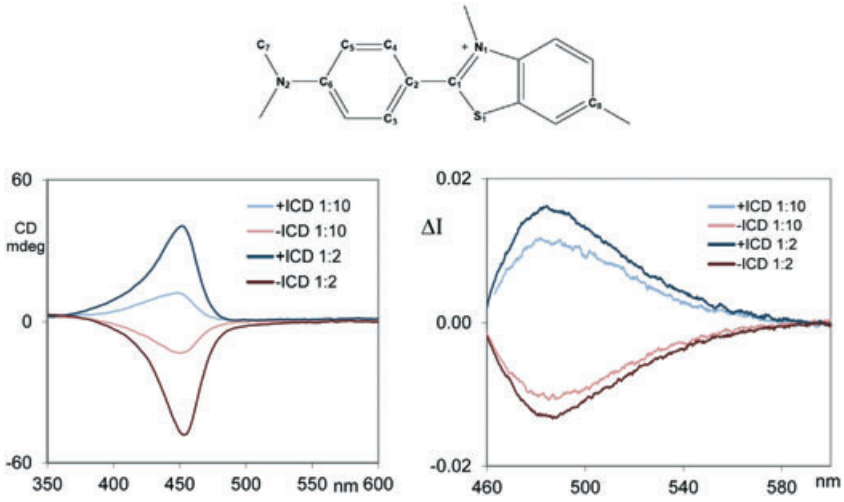

Fig. 9. Top: Thioflavin T (ThT) structure. Lower: CD spectra (left) and CPL spectra (right) of thioflavin T in presence of specially prepared insulin fibrils, winding leftwise and rightwise (+ICD and –ICD, respectively), CPL is referred to a normalized fluorescence spectrum; the legend indicates ThT:insulin ratios (data adapted from Ref. 50).

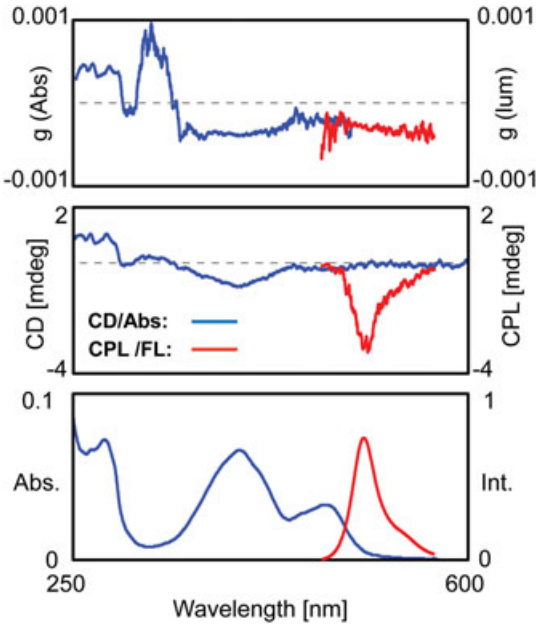

Fig. 10. Absorption (bottom, blue) and fluorescence (bottom, red), CD and CPL (center), and g_{abs} and g_{lum} spectra for wt-GFP (top) (see Ref. 35; data taken on a commercial CPL-300 Jasco apparatus). Experimental conditions: concentration: 0.03 mg/mL; excitation wavelength and SBW: 399 nm and 12 nm; emission SBW: 8 nm; cell path length: 10 mm).

intensity, and vibronic succession frequently associated with CPL (possibly with sign changes) and fluorescence activity. To this purpose we remind of the important contributions of Moffit and Moscowitz,[56] of Dekkers,[4] and of Riehl and Richardson.[9] The first TD-DFT calculations were mentioned above and were presented in Refs. 39–42 (see also Ref. 57); they have been performed by easy-to-use codes for dealing with the calculations of the electronic properties[58–60] needed to the scope, like energies and transition moments from the ground and excited states of the investigated molecules. Other useful codes for dealing with vibronic effects have been developed in the meantime.[57,61] Other more sophisticated calculations at the equation-of-motion coupled cluster singles and doubles (EOM-CCSD) level of theory have been presented by McAlexander and Crawford.[62]

The simplest way of calculating CPL spectra (not taking into account vibronic contributions) is to evaluate dipole (D_{0m}) and rotational strengths (R_{0m}) in the excited state geometry optimized by TD-DFT calculations. Fluorescence and CPL bands as function of energy E can be obtained through the following equations:

$$I = \frac{4E^3\rho(E)}{3\cdot\hbar^4\cdot c^3}D_{0m} \quad \text{and} \quad \Delta I = \frac{16E^3\rho(E)}{3\cdot\hbar^4\cdot c^3}R_{0m}$$

where $\hbar$ is the reduced Planck's constant, c is the speed of light, and $\rho(E)$ is a Gaussian band shape (equations are in c. g.s. units). The third power E dependence accounts for the fact that the way total and circularly polarized luminescence is measured is by counting the number of photons.

As an example, we comment here on our own calculations reproducing observed CPL spectra of a simple molecule like camphor,[37] since it gives a simple and vivid picture of what TD-DFT calculations are useful for. In this case two possible structures can be found in the excited state: since pyramidalization of the C=O bond occurs, with partial loss of the double bond character, two orientations

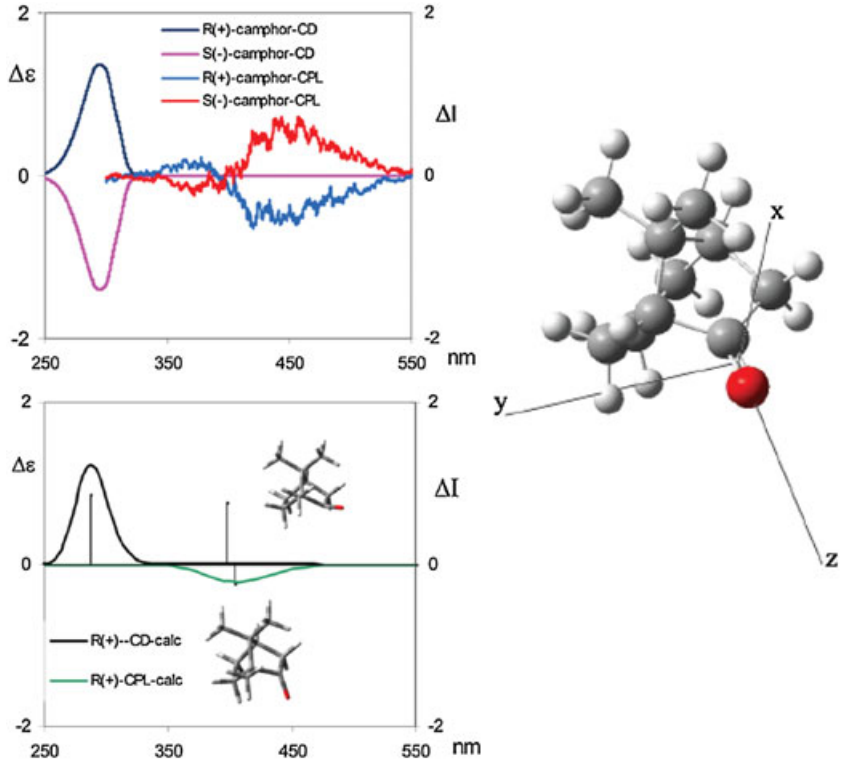

Fig. 11. Experimental CD and CPL spectra of (1*S*) and (1*R*)-camphor (top left) and calculated CD and CPL spectra (as bar and convoluted bands) of (1*R*)-camphor (lower left). On the right the structure of (1*R*)-camphor calculated by DFT, with the definition of Cartesian axes system, allowing one to perform the product – (xyz) product of atom coordinates, as required by the octant rule. (see Refs. 37,63).

are possible, below and above the CCC=O plane in the ground state. Keeping in mind the celebrated octant rule,[63] one may accept that there are two different octants in the excited state, one maintaining the rotational strength sign of the ground state and one providing opposite sign as proved and explained in Ref. 37.

Indeed, in Figure 11 not only may one appreciate how the TD-DFT complete calculations (lower left) predict two CPL bands with opposite sign, as observed in the experiment, but also one can see the definition of the Cartesian axes system centered in the C=O bond, which divides the space into octants.[63] By taking the product –(xyz), namely, the opposite

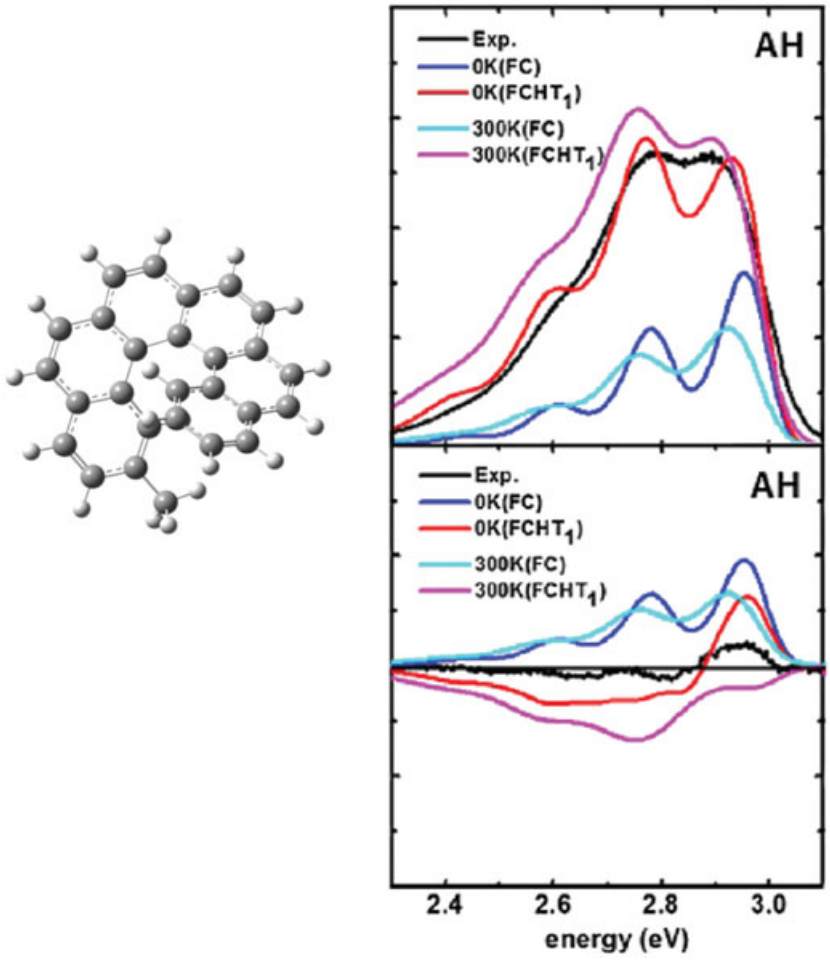

Fig. 12. Fluorescence and CPL spectra of (*M*)-2-methyl-hexahelicene: comparison of experimental (black) data with calculations at the CAM-B3LYP/TZVP level, gas phase, (shifted by 0.41 eV for the sake of comparison). (FC) Franck–Condon treatment at 0 K and 300 K, (FCHT) Franck–Condon plus Herzberg–Teller contributions at 0 K and 300 K, adiabatic Hessian approximation, derivatives of the transition electric and magnetic dipole moments taken at the equilibrium geometry of the excited state (see Ref. 70 for details).

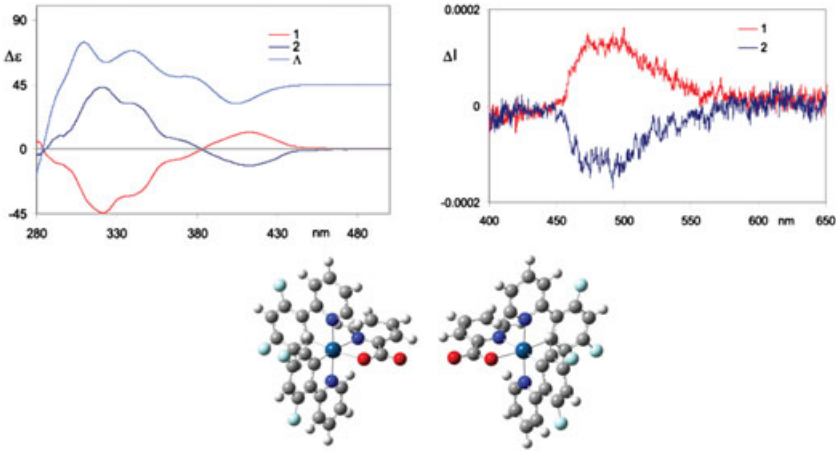

Fig. 13. Experimental CD spectra of the two enantiomers 1 and 2 of iridium (III)bis(4,6-difluorophenylpyridinato)picolinato (FIrpic) compared with the corresponding calculated CD spectrum of the Λ-enantiomer (left). Experimental CPL spectra (recorded in oxygen-free conditions) of the same compounds given on the right. DFT calculated structures are given below for Λ and Δ structures (adapted from Ref. 71). TD-DFT calculations permit the AC assignment 2 = Λ.

of the products of the coordinates of all atoms in that axis system and summing them up, one may verify that the obtained value for the ground state geometry gives the correct sign for ECD, while the corresponding values obtained for the two excited state structures give the correct signs for CPL, one opposite to the other.[37] This interpretation is complementary/concomitant to allowing for effects due to vibronic contributions that are surely present in the carbonyl transition: in fact, a change in sign through a vibronic band requires to go beyond a simple Franck-Condon approximation; in particular, the excited state two minima would require the separation of the interconversion internal coordinate from the other harmonic modes.[64]

For this instance, a case which is nontrivial for calculations is that of hexahelicenes. In Ref. 65 four cases of simple hexahelicenes are reported, comprised of hexahelicene, 2-methyl-hexahelicene, 2-Br-hexahelicene, and 4-aza-hexahelicene. All of them have weak CPL spectra but the availability of data for both enantiomers allows one to trust the data. Already in 1966 Weigang et al.[66] hypothesized that for the two nearly forbidden transitions L_a and L_b vibronic contributions should be as important as nonplanarity in generating rotational strengths: for this reason, even the sign of the observed bands is determined by vibronic contributions. Whenever calculated rotational strengths are weak, one cannot avoid considering carefully vibronic contributions to obtain a reliable interpretation. In the case of helicenes, only the presence of heteroatoms guarantees that strong enough CPL spectra be observed.[67–69] The fact that for hexahelicene and methylhexahelicene one observes differences in the vibronic structures between CD and absorption bands and between CPL and fluorescence bands and a nonmirror-image comparing absorption vs. emission bands suggests that the assumptions of Franck–Condon approximation and of the same potential energy surface in the ground and excited states are not sufficient to account for the data. In the case of these molecules one observes even an inversion of signs in the succession of vibronic features. In this situation one needs to consider Herzberg–Teller vibronic effects. We refer to Ref. 70 for a detailed and complete discussion of the alternative possible approximate methods and their comparison; here we just extract the results of Figure 12, obtained under harmonic approximation including Duschinsky effects and accounting for Franck – Condon (FC) and FC-Herzberg – Teller (FCHT) contributions at 0 K and 300 K. For the FCHT treatment we show here the results only within the adiabatic hessian (AH) approximation, for which both the initial and the final-state PESs are quadratically expanded around their own equilibrium geometries, and we consider derivatives of the transition electric and magnetic dipole moments taken at the equilibrium geometry of the excited state. Figure 12 clearly shows that the Franck–Condon terms are not sufficient to reproduce observations, but Herzberg–Teller terms are crucial. Several vibrational normal modes contribute to shaping up correctly the CPL, as well as the fluorescence, CD, and absorption calculated spectra, in a nonintuitive way.

Another challenge for circularly polarized emission spectra calculations is represented by those systems for which contributions from $T_1 \rightarrow S_0$ transitions (phosphorescence) are important. We report here an example, by presenting in Figure 13 the CPL and CD spectra of an organometallic complex called iridium (III)bis(4,6-difluorophenylpyridinato) picolinato (FIrpic),[71] one of the most investigated bis-cyclometalated iridium complexes in the context of organic light-emitting diodes.[72] On the left we show the two experimental CD spectra, and the TD-DFT calculated spectrum for one of the two enantiomers; the calculated data correlate quite well with experimental data; however, transitions involving triplet states have been invoked to contribute, due to spin-orbit coupling. On the right we provide just the experimental CPL spectra of the two enantiomers for which phosphorence effects are possible, as anticipated in Ref. 73 and a few references therein. The only attempt in the literature tackling such a problem is that of Ref. 74, where theory and a computational protocol were proposed to compute phosphorence spectra; however, a development that can treat also transition metal atoms is needed.

In conclusion, we remark how computational spectroscopy has now become an essential tool to support experimental optical spectroscopies, thus enhancing the information that one can gain from experiments. Even though calculations of CPL spectra are less widespread than for other more common techniques, TD-DFT gives quite reliable results. Comparison of CPL experimental and calculated spectra give valuable information regarding the excited electronic state from which emission takes place. The examples reported here point out difficult but interesting questions that the literature is now affording and developing, particularly the treatment of vibronic contributions to reproduce and understand "complicated" band shapes and calculations of spin forbidden transitions.

CONCLUSIONS

In this review we have reported on the status of the experimental advancement of CPL. To this end and to testify to a solidly increased interest in CPL spectroscopy, we wish to report that recently even ROA (Raman Optical Activity) apparatuses were employed to detect CPL.[75] Furthermore, limiting ourselves to the case of organic molecules or organic molecule-based molecular systems (for which $|g_{lum}|$ has a value of at most 10^{-2}; see the review by de la Moya et al.[13] and not of ~1 as for lanthanide complexes), we have presented the most interesting applications of CPL to investigations in the material science and biology fields. Finally, we considered the computational results for CPL, which are increasing in number and reliability, since the implementation and widespread use of DFT protocols.

APPENDIX A

In Figure A1 we report the statistics of articles dealing with or employing the CPL technique.

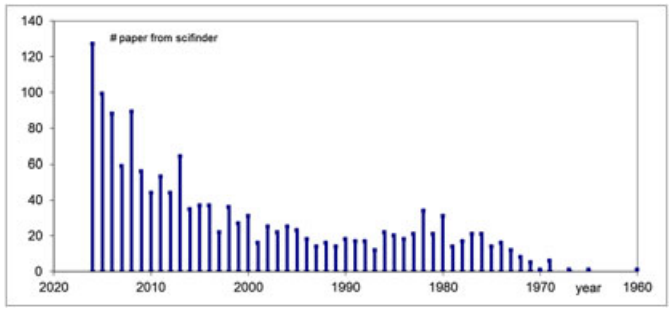

Fig. 14. Number of published articles per year, in which CPL is employed, from 1960 to 2016 (source: SciFinder-ACS).

ACKNOWLEDGMENTS

We thank Professor Francesco Sannicolò, Università degli Study di Milano, Italy and Doctor Thierry Brotin, C.N.R.S., Lyon, France, for providing some of the samples employed in the experiments presented in Figures 6 and 7.

LITERATURE CITED

1. a) Samoilov BN. Luminescence from a chiral crystal of sodium uranyl acetate. J Exp Theor Phys 1948; 18: 1030–1040.
   b) Agranovich VM. The theory of circular dichroism in crystals. Fizika Tverdogo Tela (Sankt-Peterburg) 1960; 2: 1197–1199.
2. Emeis CA, Oosterhoff LJ. Emission of circularly-polarized radiation by optically-active compounds. Chem Phys Lett 1967; 1: 129–132.
3. Dekkers HPJM, Closs LE. The optical activity of low-symmetry ketones in absorption and emission. J Am Chem Soc 1976; 98: 2210–2219.
4. Dekkers HPJM. Circularly polarized luminescence: a probe for chirality in the excited state. In: Berova N, Nakanishi K, Woody RW, editors. Circular dichroism: principles and applications, 2nd ed. John Wiley & Sons: New York; 2000. p 185–215.
5. Steinberg IZ, Gafni A. Sensitive instrument for the study of circular polarization of luminescence. Rev Sci Instrum 1972; 43: 409–413.
6. a) Luk CK, Richardson FS. Circularly polarized luminescence spectrum of camphorquinone. J Am Chem Soc 1974; 96: 2006–2007.
   b) Richardson FS, Riehl JP. Circularly polarized luminescence spectroscopy. Chem Rev 1977; 77: 773–792.
7. Richardson FS, Riehl JP. Circularly polarized luminescence spectroscopy. Chem Rev 1977; 77: 773–792.
8. Brittain HG. Excited-state optical activity. In: Molecular luminescence spectroscopy methods and applications. Part I. Wiley Interscience: New York; 1985 .Chapter 6
9. Riehl JP, Richardson FS. Circularly polarized luminescence spectroscopy. Chem Rev 1986; 86: 1–16.
10. Riehl JP, Muller FG. Circularly polarized luminescence spectroscopy and emission-detected circular dichroism. In: Berova N, Polavarapu PL, Nakanishi K, Woody RW, editors. Comprehensive chiroptical spectroscopy, Vol. 1. John Wiley & Sons: New York; 2012. p 65–90.
11. Sisido M, Egusa S, Okamoto A, Imanishi Y. Circularly polarized fluorescence of aromatic poly(α-amino acids). J Am Chem Soc 1983; 105: 3351–3352.
12. Zinna F, Di Bari L. Lanthanide circularly polarized luminescence: bases and applications. Chirality 2015; 27: 1–13.
13. Sànchez-Carnerero E, Agarrabeitia AR, Moreno F, Maroto BL, Muller G, Ortiz MJ, de la Moya S. Circularly polarized luminescence from simple organic molecules. Chem Eur J 2015; 21: 13488–13500.
14. Castiglioni E, Abbate S, Lebon F, Longhi G. Chiroptical spectroscopic techniques based on fluorescence. Methods Appl Fluoresc 2014; 2: 024006 .7p
15. Wynberg H, Meijer EW, Hummelen JC, Dekkers HPJM, Schippers PH, Carlson AD. Circular polarization observed in bioluminescence. Nature 1980; 286: 641–642.
16. Naito M, Iwahori K, Miura A, Yamane M, Yamashita Y. Fluorescence and CPL spectra of CdS@Ferritin quantum dots before and after laser etching. Angew Chem Int Ed 2010; 49: 7006–7009.
17. Tohgha U, Deol KK, Porter AG, Bartko SG, Choi JK, Leonard BM, Varga K, Kubelka J, Muller G, Balaz M. Ligand induced circular dichroism and circularly polarized luminescence in CdSe quantum dots. ACS Nano 2013; 7: 11094–11102.
18. Kimoto T, Kajima N, Fujiki M, Imai Y. CPL and PL spectra of S and R binaphtols as dopants of PMMA. Chem Asian J 2012; 7: 2836–2841.
19. Maeda H, Bando Y, Shimomura K, Yamada I, Naito M, Nobusawa K, Tsumatori H, Kawai T. Chemical-stimuli-controllable circularly polarized luminescence from anion-responsive π-conjugated molecules. J Am Chem Soc 2011; 133: 9266–9269.
20. Maeda H, Bando Y. Recent progress in research on stimuli-responsive circularly polarized luminescence based on π-conjugated molecules. Pure Appl Chem 2013; 85: 1967–1978.
21. Isla H, Srebro-Hooper M, Vanthuyne MJN, Roisnel T, Lunkley JL, Muller G, Williams JAG, Autschbach J, Crassous J. Conformational changes and chiroptical switching of enantiopure bis-helicenic terpyridine upon Zn^{2+} binding. Chem Commun 2016; 52: 5932–5935.
22. Saleh N, Moore B, Srebro M, Vanthuyne N, Toupet L, Williams JAG, Roussel C, Deol KK, Muller G, Autschbach J, Crassous J. Acid/base-triggered switching of circularly polarized luminescence and electronic circular dichroism in organic and organometallic helicenes. Chem Eur J 2015; 21: 1673–1681.
23. Morcillo SP, Miguel D, Alvarez de Cienfuegos L, Justicia J, Abbate S, Castiglioni E, Bour C, Ribagorda M, Cardenas DJ, Paredes JM, Crovetto J, Choquesillo-Lazarte D, Mota AJ, Carreño MC, Longhi G, Cuerva JM. Stapled helical o-OPE foldamers as new circularly polarized luminescence emitters based on carbophilic interactions with Ag(I)-sensitivity. Chem Sci 2016. DOI:10.1039/c6sc01808d.
24. Amako T, Nakabayashi K, Mori T, Inoue Y, Fujiki M, Imai Y. Sign inversion of circularly polarized luminescence by geometry manipulation of four naphthalene units introduced into a tartaric acid scaffold. Chem Commun 2014; 50: 12836–12839.
25. Okano K, Taguchi M, Fujiki M, Yamashita T. Circularly polarized luminescence of rhodamine B in a supramolecular chiral medium formed by a vortex flow. Angew Chem Int Ed 2011; 50: 12474–12477.
26. Fujiki M, Yoshida K, Suzuki N, Rahim NAA, Jalil JA. Tempo-spatial chirogenesis. Limonene-induced mirror symmetry breaking of single bond Si bond polymers during aggregation in chiral fluidic media. J Photochem Photobiol A Chem 2016. DOI:10.1016/j.jphotochem.2016.01.027.
27. Kumar J, Nakashima T, Kawai T. Circularly polarized luminescence in chiral molecules and supramolecular assemblies. J Phys Chem Lett 2015; 6: 3445–3452.
28. Yamamoto Y, Sakai H, Yuasa J, Araki Y, Wada T, Sakanoue T, Takenobu T, Kawai T, Hasobe T. Controlled excited-state dynamics and enhanced fluorescence property of tetrasulfone[9]helicene by a simple synthetic process. J Phys Chem C 2016; 120: 7421–7427.
29. Watanabe K, Osaka I, Yorozuya S, Akagi K. Helically π-stacked thiophene-based copolymers with circularly polarized fluorescence: high dissymmetry factors enhanced by self- ordering in chiral nematic liquid crystal phase. Chem Mater 2012; 24: 1011–1024.
30. Hirata S, Vacha M. Circularly polarized persistent room-temperature phosphorescence from metal-free chiral aromatics in air. J Phys Chem Lett 2016; 7: 1539–1545.
31. Gon M, Morisaki Y, Sawada R, Chujo Y. Synthesis of optically active, X-shaped, conjugated compounds and dendrimers based on planar chiral [2.2]paracyclophane, leading to highly emissive circularly polarized luminescence. Chem Eur J 2016. DOI:10.1002/chem.201504270.
32. Castiglioni E, Abbate S, Longhi G. Revisting with updated hardware and old spectroscopic technique: circularly polarized luminescence. Appl Spectrosc 2010; 64: 1416–1419.
33. Sutherland JC. Dichrometer errors resulting from large signals or improper modulator phasing. Chirality 2012; 24: 706–717.
34. Blok PML, Dekkers HPJM. Measurement of the circular polarization of the luminescence of photoselected samples under artefact-free conditions. Appl Spectrosc 1990; 44: 305–309.
35. Kondo Y, Watanabe M, Akao K, Koshoubu J, Nagamori K. Development and applications of new circularly polarized luminescence spectrometer. Oral Note O-17 presented at Molecular Chirality Asia 2016, Osaka University, April 20–222016.
36. Castiglioni E, Abbate S, Lebon F, Longhi G. Ultraviolet, circular dichroism, fluorescence, and circularly polarized luminescence spectra of regioregular poly-[3-((S)-2-methylbutyl)-thiophene] in solution. Chirality 2012; 24: 725–730.
37. Longhi G, Castiglioni E, Abbate S, Lebon F, Lightner DA. Experimental and calculated CPL spectra and related spectroscopic data of camphor and other simple chiral bicyclic ketones. Chirality 2013; 25: 589–599.
38. Valeur B. Molecular fluorescence. Principles and applications. Wiley-VCH: Weinheim, Germany; 2001.
39. Barone V, Baiardi A, Bloino J. New developments of a multifrequency virtual spectrometer: stereo-electronic, dynamical and environmental effects on chiroptical spectra. Chirality 2014; 26: 588–600.
40. Santoro F, Jacquemin D. Going beyond the vertical approximation with time dependent density functional theory. wireswileycom/compmolsci 2016; 1–27.
41. Pritchard B, Autschbach J. Calculation of vibrationally resolved circularly polarized luminescence of d-camphorquinone and (S,S)-trans-bhydrindanone. Chem Phys Chem 2010; 11: 2409–2415.

42. Pecul M, Ruud K. The optical activity of beta, gamma-enones in ground and excited states using circular dichroism and circularly polarized luminescence. Phys Chem Chem Phys 2011; 13: 643–650.
43. Longhi G, Abbate S, Mazzeo G, Castiglioni E, Mussini PR, Benincori T, Martinazzo R, Sannicolò F. Structural and optical properties of inherently chiral polythiophenes: a combined CD-electrochemistry, circularly polarized luminescence and TDDFT investigation. J Phys Chem C 2014; 118: 16019–16027.
44. Sannicolò F, Arnaboldi S, Benincori T, Bonometti V, Cirilli R, Dunsh L, Kutner W, Longhi G, Mussini PR, Panigati M, Pierini M, Rizzo S. Potential-driven chirality manifestations and impressive enantioselectivity by inherently chiral electroactive organic films. Angew Chem Int Ed 2014; 53: 2623–2627.
45. Sannicolò F, Mussini PR, Benincori T, Cirilli R, Abbate S, Arnaboldi S, Casolo S, Castiglioni E, Longhi G, Martinazzo R, Panigati M, Pappini M, Quartapelle Procopio E, Rizzo S. Inherently chiral macrocyclic oligothiophenes: easily accessible electrosensitive cavities with outstanding enantioselection performances. Chem Eur J 2014; 20: 15298–15302.
46. Cavagnat D, Buffeteau T, Brotin T. Synthesis and chiroptical properties of cryptophanes having C1-symmetry. J Org Chem 2008; 73: 66–75.
47. Bouchet A, Brotin T, Linares M, Ågren H, Cavagnat D, Buffeteau T. Conformational effects induced by guest encapsulation in an enantiopure water-soluble cryptophane. J Org Chem 2011; 76: 1372–1383.
48. Nieto-Ortega B, García F, Longhi G, Castiglioni E, Calbo J, Abbate S, López Navarrete JT, Ramírez FJ, Ortí E, Sánchez L, Casado J. On the handedness of helical aggregates of C3 tricarboxamides: a multichiroptical characterization. Chem Commun 2015; 51: 9781–9784.
49. Pollack GH. Cells, gels and the engines of life. (A new, unifying approach to cell function), 1st ed. Ebner and Sons Publishers: Seattle; 2001. p 305.
50. Dzwolak D, Loksztejn A, Galinska-Rakoczy A, Adachi R, Goto Y, Rupnicki L. Conformational indeterminism in protein misfolding: chiral amplification on amyloidogenic pathway of insulin. J Am Chem Soc 2007; 129: 7517–7522.
51. Rybicka A, Longhi G, Castiglioni E, Abbate S, Dzwolak W, Babenko V, Pecul M. Thioflavin T: electronic circular dichroism and circularly polarized luminescence induced by amyloid fibrils. Chem Phys Chem 2016. DOI:10.1002/cphc.201600235.
52. Dzwolack W, Pecul M. Chiral bias of amyloid fibrils revealed by the twisted conformation of Thioflavin T: an induced circular dichroism/DFT study. FEBS Lett 2005; 579: 6601–6603.
53. Chalfie M, Kain SR. Green fluorescent protein: properties, applications and protocols. John Wiley & Sons: New York; 2005.
54. Day RN, Davidson MW. The fluorescent protein revolution. CRC Press: Chicago; 2014.
55. Visser NV, Hinka MW, Borsta JW, van der Krogta GNM, Visser AJWG. Circular dichroism spectroscopy of fluorescent proteins. FEBS Lett 2002; 521: 31–35.
56. Moffit W, Moscowitz A. Optical activity in absorbing media. J Chem Phys 1959; 30: 648–660.
57. Barone V. The virtual multifrequency spectrometer: a new paradigm for spectroscopy. WIREs Comput Mol Sci 2016; 6: 86–110.
58. Gaussian 09, Revision A.02, Frisch MJ, Trucks GW, Schlegel HB, Scuseria GE, Robb MA, Cheeseman JR, Scalmani G, Barone V, Mennucci B, Petersson GA, Nakatsuji H, Caricato M, X L, Hratchian HP, Izmaylov AF, Bloino J, Zheng G, Sonnenberg JL, Hada M, Ehara M, Toyota K, Fukuda R, Hasegawa J, Ishida M, Nakajima T, Honda Y, Kitao O, Nakai H, Vreven T, Montgomery JA Jr, Peralta JE, Ogliaro F, Bearpark M, Heyd JJ, Brothers E, Kudin KN, Staroverov VN, Kobayashi R, Normand J, Raghavachari K, Rendell A, Burant JC, Iyengar SS, Tomasi J, Cossi M, Rega N, Millam JM, Klene M, Knox JE, Cross JB, Bakken V, Adamo C, Jaramillo J, Gomperts R, Stratmann RE, Yazyev O, Austin AJ, Cammi R, Pomelli C, Ochterski JW, Martin RL, Morokuma K, Zakrzewski VG, Voth G, Salvador P, Dannenberg S, Dapprich S, Daniels AD, Farkas Ö, Foresman JB, Ortiz JV, Cioslowski J, Fox DJ. Gaussian. Gaussian, Inc.: Wallingford CT; 2009.
59. Dalton 2016, Aidas K, Angeli C, Bak KL, Bakken V, Bast R, Boman L, Christiansen O, Cimiraglia R, Coriani S, Cukras J, Dahle P, Dalskov EK, Enevoldsen T, Eriksen JJ, Faber R, Fernández B, Ferrighi L, Fliegl H, Frediani L, Gao B, Hald K, Halkier A, Hansen FBK, Hedegård ED, Hättig C, Heiberg H, Helgaker T, Hennum AC, Hettema H, Hjertenæs E, Iozzi MF, Jansik B, Jensen HJAa, Jonsson D, Jørgensen P, Kami'nski M, Kauczor J, Kirpekar S, Klopper W, Knecht S, Kobayashi R, Koch H, Kongsted J, Ligabue A, List NH, Lutnæs OB, Melo JI, Mikkelsen KV, Myhre RH, Neiss C, Nielsen CB, Norman P, Olsen J, Olsen JMH, Osted A, Packer MJ, Pawlowski F, Pedersen MN, Pedersen TB, Provasi PF, Rinkevicius Z, Rudberg E, Ruden TA, Ruud K, Salek P, Samson CCM, Sánchez de Merás A, Saue T, Sauer SPA, Schimmelpfennig B, Sneskov K, Steindal AH, Steinmann C, Sylvester-Hvid KO, Taylor PR, Teale AM, Tew DP, Vahtras O, Wilson DJD, Ågren H. 2016; http://www.daltonprogram.org/www/resources/dalton2016manual.pdf
60. Furche F, Ahlrichs R, Hättig C, Klopper W, Sierka M, Weigend F. TURBOmole. WIREs Comput Mol Sci 2013. DOI:10.1002/wcms.1162.
61. Santoro F. FC classes, a Fortran 77 code, development version. The standard version of the code can be downloaded at http://www.pi.iccom.cnr.it/fcclasses, last accessed March 5 2015.
62. McAlexander HR, Crawford TD. Simulation of circularly polarized luminescence spectra using coupled cluster theory. J Chem Phys 2015; 142: 154101.
63. Lightner DA, Gurst JE. Organic conformational analysis and stereochemistry from circular dichroism spectroscopy. John Wiley & Sons: New York; 2000 .Chapter 4
64. Scafato P, Caprioli F, Pisani L, Padula D, Santoro F, Mazzeo G, Abbate S, Lebon F, Longhi G. Combined use of three forms of chiroptical spectroscopies in the study of the absolute configuration and conformational properties of 3-phenylcyclopentanone, 3-phenylcyclohexanone, and 3-phenylcycloheptanone. Tetrahedron 2013; 69: 10752–10762.
65. Abbate S, Longhi G, Lebon F, Castiglioni E, Superchi S, Pisani L, Fontana F, Torricelli F, Caronna T, Villani C, Sabia R, Tommasini M, Lucotti A, Mendola D, Mele A, Lightner DA. Helical sense-responsive and substituent-sensitive features in vibrational and electronic circular dichroism, in circularly polarized luminescence and in Raman spectra of some simple optically active hexahelicenes. J Phys Chem C 2014; 118: 1682–1695.
66. Weigang OE, Turner JA, Trouard PA. Emission polarization and circular dichroism of hexahelicene. J Chem Phys 1966; 45: 1126–1134.
67. Longhi G, Castiglioni E, Villani C, Sabia R, Menichetti S, Viglianisi C, Devlin F, Abbate S. Chiroptical properties of the ground and excited states of two thia-bridged triarylamine heterohelicenes. J Photobiol Photochem A: Chemistry 2016. DOI:10.1016/j.jphotochem.2015.12.011.
68. Field JE, Muller G, Riehl JP, Venkataraman D. Circularly polarized luminescence from bridged triarylamine helicenes. J Am Chem Soc 2003; 125: 11808–11809.
69. Shen C, Anger E, Srebro M, Vanthuyne N, Deol KK, Jefferson TD, Muller G, Williams JAG, Toupet L, Roussel C, Autschbach J, Réau R, Crassous J. Straightforward access to mono- and bis-cycloplatinated helicenes displaying circularly polarized phosphorescence by using crystallization resolution methods. Chem Sci 2014; 5: 1915–1927.
70. Liu Y, Cerezo J, Mazzeo G, Lin N, Zhao X, Longhi G, Abbate S, Santoro F. Vibronic coupling explains the different aspect of electronic circular dichroism and of circularly polarized luminescence spectra of hexahelicenes. J Chem Theor Comput 2016; 12: 2799–2819.
71. Citti C, Battisti UM, Ciccarella G, Maiorano V, Gigli G, Abbate S, Mazzeo G, Castiglioni E, Longhi G, Cannazza G. Analytical and preparative enantioseparation and main chiroptical properties of Iridium (III)bis(4,6-difluorophenylpyridinato)picolinato (FIrpic). J Chromath A 2016. DOI:10.1016/j.chroma.2016.05.059.
72. Li T-L, Jing Y-M, Liu X, Zhap Y, Shi L, Tang Z, Zheng Y-M, Zuo J-L. Circularly polarised phosphorescent photoluminescence of iridium complexes. Sci Rep 2015; 14912: 1–9.
73. Mazzeo G, Fusè M, Longhi G, Rimoldi I, Cesarotti E, Crispini A, Abbate S. Vibrational circular dichroism and chiroptical properties of chiral Ir(III) luminescent complexes. Dalton Trans 2016; 45: 992–999.
74. Kaminski M, Cukras J, Pecul M, Rizzo A, Coriani S. A computational protocol for the study of circularly polarized phosphorescence and circular dichroism in spin-forbidden absorption. Phys Chem Chem Phys 2015; 7: 19079–19086.
75. Wu T, Kapitàn J, Bour P. Detection of circularly polarized luminescence of a Cs-EuIII complex in Raman optical activity experiments. Angew Chem Int Ed 2015; 54: 14933–14936.